

New approach to superresolution

Haifeng Wang

Fuxi Gan, FELLOW SPIE

Shanghai Institute of Optics and Fine
Mechanics

Chinese Academy of Sciences
201800 Shanghai, China

E-mail: hfwang2@yahoo.com

Abstract. We propose a new method to increase the resolution of an optical system by modifying part of the spatial-frequency spectrum, viz., displacing the lower-frequency light to a high-frequency band, which makes the central maximum in the diffraction pattern narrower and increases the depth of focus. Simulation results show that this kind of apodizer (the term apodization was originally used to describe ways to reduce the sidelobes of the PSF, but in this paper, we use it in a wider sense) is superior to the phase-shifting ones. © 2001 Society of Photo-Optical Instrumentation Engineers. [DOI: 10.1117/1.1359207]

Subject terms: superresolution; spatial frequency; half-width ratio; center-peak intensity ratio; relative sidelobe peak intensity.

Paper 990505 received Dec. 16, 1999; revised manuscript received June 12, 2000; accepted for publication Dec. 5, 2000.

1 Introduction

It is known that superresolution techniques can be divided into two categories.¹ The first, which increases the generalized Rayleigh resolution but does not extend the spatial cutoff frequency, is termed ultraresolution. Ultraresolution may be achieved by optical methods,²⁻⁶ viz., by modifying the lens aperture with a suitable filter or by expanding the pupil function in some complete set of functions with arbitrary coefficients and then adjusting the coefficients to approximate a prespecified point-spread function. The second category of superresolution techniques increases the spatial cutoff frequency of an optical system.^{7,8} In this paper we proposed a new method to attain superresolution by modifying the spatial frequency of the light, viz., displacing the lower-spatial-frequency light to a high-spatial-frequency band, but not increasing the cutoff frequency.

2 The Principle of Operation of the System

Figure 1 shows that the apodizer changes the incident light beam into a collimated annular beam, i.e., the lower-spatial-frequency light has been displaced to a high-frequency band. This apodizer is actually a beam shaper.⁹⁻¹¹ Suppose that the ring is of uniform intensity; now this optical system is comparable with an optical system with annular aperture.¹² Decreasing the ring width is equivalent to increasing the inner radius of the annular aperture.

Now, let the focal length of the objective lens be F ,⁴ the numerical aperture be NA , the wavelength be λ , the coordinates of the objective-lens pupil plane be (X, Y) , and the coordinates of the beam waist plane be (x, y) . We define the following:

$$r = \frac{1}{NA \cdot F} (X^2 + Y^2)^{1/2}, \quad (1)$$

$$R = (x^2 + y^2)^{1/2}. \quad (2)$$

When a light source of uniform intensity distribution is applied, the normalized amplitude distribution in the beam waist plane becomes

$$G\left(2\pi \frac{NA}{\lambda} R\right) = 2 \int_0^1 r g(r) J_0\left(2\pi \frac{NA}{\lambda} Rr\right) dr, \quad (3)$$

where $g(r)$ represent the transmission function of the pupil plane. If we substitute ρ for $2\pi (NA/\lambda) R$, we get the following transformation:

$$G(\rho) = 2 \int_0^1 r g(r) J_0(\rho r) dr. \quad (4)$$

For a center-obstructed system, the obstruction ratio is denoted as ε . The transmission function of the pupil plane, $g(r)$, can be written as follows:

$$g(r) = \begin{cases} 0 & \text{for } 0 \leq r < \varepsilon, \\ 1 & \text{for } \varepsilon \leq r \leq 1. \end{cases}$$

Thus, the transformation can be written as

$$G(\rho) = 2 \int_{\varepsilon}^1 r J_0(\rho r) dr = \frac{2}{\rho} [J_1(\rho) - \varepsilon J_1(\varepsilon \rho)], \quad (5)$$

For small values of ρ , we use Eq. (a) in the Appendix⁴ to obtain an approximate formula to third order:

$$G(\rho) = \frac{1}{8} [8(1 - \varepsilon^2) - \rho^2(1 - \varepsilon^4)]. \quad (6)$$

The center-peak intensity ratio is

$$S = [G_{\varepsilon \neq 0}(0)/G_{\varepsilon=0}(0)]^2 = (1 - \varepsilon^2)^2. \quad (7)$$

If we call the half-width ratio H , then Eqs. (6) and (7) yield the following equation connecting H and S :

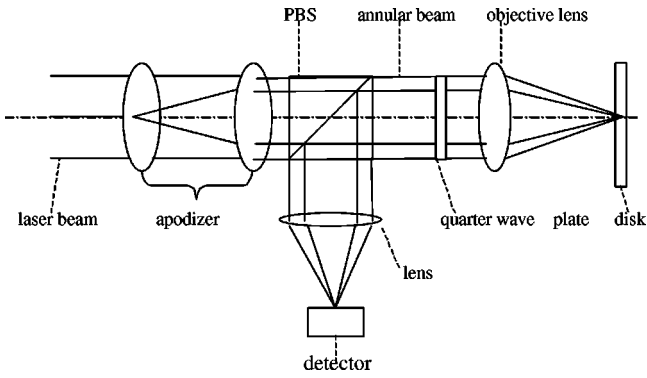


Fig. 1 System setup. The apodizer changes the incident light beam into a collimated annular beam; then the annular beam is converged by an optical lens.

$$H^2 = \frac{1}{2 - S^{1/2}}. \tag{8}$$

The normalized amplitude distribution along the axis is

$$G(u) = 2 \int_{\epsilon}^1 \exp\left(-\frac{1}{2} iur^2\right) r dr = \frac{2}{iu} \left[\exp\left(-\frac{1}{2} iu\right) - \exp\left(-\frac{1}{2} iu\epsilon^2\right) \right], \tag{9}$$

where $u = (2\pi/\lambda)(Na)^2z$. The normalized intensity along the axis is written as

$$I = |G(u)|^2 = (1 - \epsilon^2)^2 \text{sinc}^2\left[\frac{1}{4}u(1 - \epsilon^2)\right], \tag{10}$$

For $\epsilon = 0$,

$$I = \text{sinc}^2\left(\frac{1}{4}u\right). \tag{11}$$

Let $1/(1 - \epsilon^2) = n$. It is clear that the focal depth is increased n -fold. But with fixed obstruction ratio ϵ , an n -fold gain in focal depth involves precisely an n -fold loss of light.

For the proposed optical system, the light in the central part of the aperture is not obstructed, but displaced to the outer ring, so that the energy is transferred by the system without loss. Suppose the amplitude of the apodized ring is A ; then the intensity distribution of the apodized beam can be expressed as

$$I(r) = \begin{cases} 0 & (0 \leq r < \epsilon), \\ A^2 & (\epsilon \leq r \leq 1). \end{cases} \tag{12}$$

According to the energy conservation law, we get

$$E = 2\pi \int_{\epsilon}^1 A^2 r dr = 2\pi \int_0^1 r dr. \tag{14}$$

Thus we obtain

$$A = \frac{1}{\sqrt{1 - \epsilon}}. \tag{15}$$

The normalized amplitude distribution in the beam waist plane becomes

$$G(\rho) = 2 \int_{\epsilon}^1 Ar J_0(\rho r) dr = \frac{2}{\rho\sqrt{1 - \epsilon^2}} [J_1(\rho) - \epsilon J_1(\epsilon\rho)] = \frac{1}{8\sqrt{1 - \epsilon}} [8(1 - \epsilon^2) - \rho^2(1 - \epsilon^4)]. \tag{16}$$

The center-peak intensity ratio is

$$S_1 = |G_{\epsilon \neq 0}(0)/G_{\epsilon = 0}(0)|^2 = 1 - \epsilon^2. \tag{17}$$

Let H_1 be the half-width ratio. From Eqs. (16) and (17), we obtain the following equation connecting H_1 and S_1 :

$$H_1^2 = \frac{1}{2 - S_1}. \tag{18}$$

The amplitude along the axis is

$$G_1(u) = 2 \int_{\epsilon}^1 A \exp\left(-\frac{1}{2} iur^2\right) r dr = \frac{2}{iu} \left[\exp\left(-\frac{1}{2} iu\right) - \exp\left(-\frac{1}{2} iu\epsilon^2\right) \right] \frac{1}{\sqrt{1 - \epsilon^2}}. \tag{19}$$

Accordingly, the intensity along the axis is

$$I_1(u) = |G_1(u)|^2 = (1 - \epsilon^2) \text{sinc}^2\left[\frac{1}{4}u(1 - \epsilon^2)\right]. \tag{20}$$

Comparison of Eqs. (10), (11), and (20) shows that the focal length is also increased n -fold, and the intensity along the axis is n times that in the obstructed system. Comparison of Eqs. (7) and (17) shows that for the same ϵ , the center-peak intensity ratio of the apodized system is n times that of the obstructed system. Comparison of Eqs. (8) and (18) shows that, for the same half-width ratio, the center-peak intensity of the apodized system is n times that of the obstructed system.

3 The Simulation Results

The radial and the axial performance of the obstructed, the unobstructed, and the apodized system are shown in Fig. 2 and Fig. 3.

In Fig. 2, the dashed curve corresponds to the radial performance of the center-obstructed system, where the obstruction ratio is $\epsilon = 0.85$. The solid curve corresponds to the radial performance of the apodized system, where the inner radius of the annular beam is $\epsilon = 0.85$. And the dotted curve corresponds to the performance of the system without apodization and obstruction. It can be seen that the center

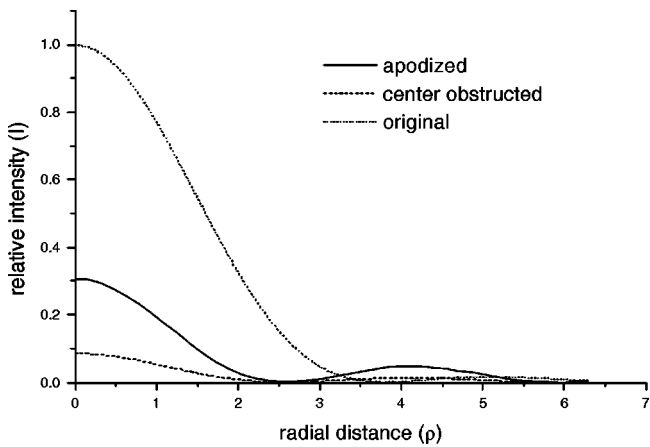


Fig. 2 Radial behavior. The dashed curve corresponds to the radial performance of the center-obstructed system, where the obstruction ratio is $\epsilon=0.85$. The solid curve corresponds to the radial performance of the apodized system, where the inner radius of the annular beam is $\epsilon=0.85$. The dotted curve corresponds to the performance of the system without apodization and obstruction.

peak intensities of the proposed system and the obstructed system are 0.306 and 0.085, respectively. The center peak intensity of the apodized system is 3.6 times that of the obstructed system.

The apodized curve can also be obtained by multiplying the obstructed curve by a constant factor [compare Eqs. (5) and (16)]. That means the two curves have a common normalized curve. So they have the same relative sidelobe peak intensity (defined as the ratio of the sidelobe peak intensity to the main-lobe peak intensity) and half-width ratio.

In Fig. 3 the dashed curve corresponds to the axial performance of the obstructed system with an obstruction ratio $\epsilon=0.85$. The solid curve corresponds to the axial performance of the apodized system where the inner radius of the annular beam is $\epsilon=0.85$. The dotted curve corresponds to

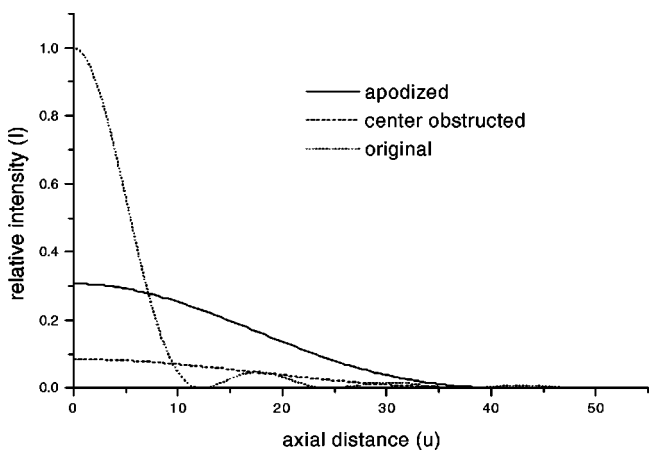


Fig. 3 Axial behavior. The dashed curve corresponds to the axial performance of the obstructed system with an obstruction ratio $\epsilon=0.85$. The solid curve corresponds to the axial performance of the apodized system where the inner radius of the annular beam is $\epsilon=0.85$. The dotted curve corresponds to the axial performance of the system without obstruction and apodization.

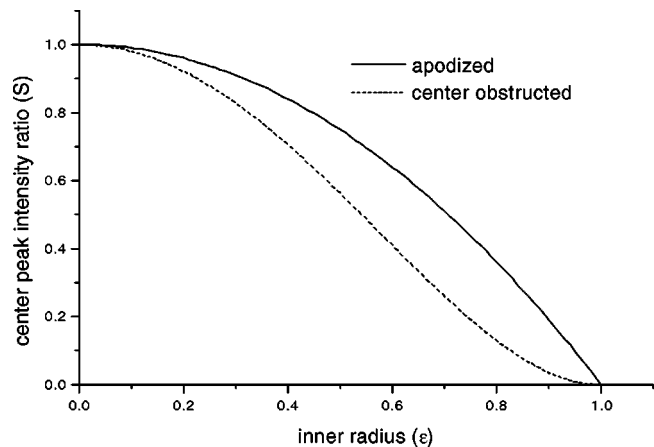


Fig. 4 Center-peak intensity versus obstruction ratio. The solid curve corresponds to the apodized system, and the dashed curve corresponds to the obstructed system.

the axial performance of the system without obstruction and apodization. The center peak intensities of the obstructed system and the apodized system are equal to that shown in Fig. 2. The intensity of the apodized system is again 3.6 times that of the obstructed system. If we take the distance where the axial intensity drops to 80% of the peak intensity as the focal depth, the focal depths of the apodized and unapodized systems are 10.84 and 3.17, respectively. The focal depth of the apodized system is 3.42 times that of the unapodized system, but it is the same as that of the obstructed system.

Figure 4 shows the center peak intensity versus ϵ of the obstructed system and the apodized system. The solid curve corresponds to the apodized system, and the dashed curve corresponds to the obstructed system. For the same ϵ , the center peak intensity is n times that of the obstructed system. For $\epsilon=0.85$, $n=3.6$; for $\epsilon=0.95$, $n=10.25$.

Figure 5 shows the half-width ratio versus the center peak intensity ratio. The dashed curve corresponds to the obstructed system, and the solid curve corresponds to the apodized system. It is easy to see that for the same half-width ratio, the apodized system has a higher center-peak

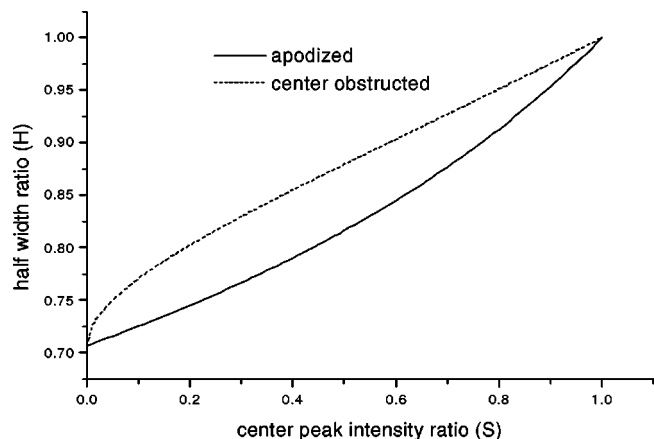


Fig. 5 Half-width ratio versus center-peak intensity ratio. The dashed curve corresponds to the obstructed system, and the solid curve corresponds to the apodized system.

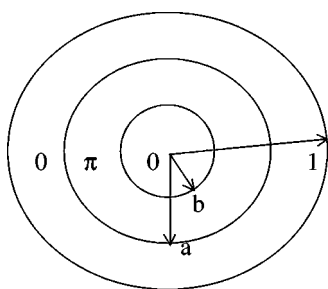


Fig. 6 Structure of the three-part phase-shifting apodizer.

intensity. For $H=0.75$, the obstructed system has a center-peak intensity of 0.0494, while the apodized system has a center-peak intensity of 0.2222, improved 4.5-fold.

4 Discussion

It is known that compared with the phase-shift apodization, the center-obstructed system has a lower relative sidelobe peak intensity.⁴ Our apodized system also has this trait. Unlike other superresolution methods, this one achieves superresolution by displacing the lower-spatial-frequency light to a high-spatial-frequency band. Simulation results have shown that this kind of apodizer is superior to phase-shifting ones.

One way to design this kind of apodizer is through binary optics.⁹⁻¹¹ The apodizer is composed of two phase elements with a suitable distance between them. The first one changes the intensity distribution; the second one corrects the phase. Let the distance between the two elements be z . Then the phase distributions of the two elements can be designed as follows:

$$\varphi_1(r) = \int_0^1 \frac{2\pi}{\lambda} \frac{r^2(1-\varepsilon^2) + \varepsilon^2 - r^{1/2}}{z} dr \quad (21)$$

$$\varphi_2(r) = \int_0^1 \frac{2\pi}{\lambda} \frac{r - [(r - \varepsilon^2)/(1 - \varepsilon)]^{1/2}}{z} dr \quad (22)$$

Equations (21) and (22) are initial expressions. They can be optimized with many methods.⁹

Now, let us compare the superresolution effect of the proposed method with that of the phase-shifting method.

Figure 6 shows the structure of a three-part phase-shifting apodizer. The apodizer is optimized by proper selection of the radii b and a . If the center peak intensity is kept unchanged, increasing the inner radius b can bring down the first sidelobe peak intensity, but this is gained at the expense of a decreased half-width ratio and increased second-sidelobe intensity. If the sidelobe intensity is not taken into consideration, for a certain center-peak intensity, $b=0$ corresponds to the minimum half-width ratio, that is to say, for a certain half-width ratio, $b=0$ corresponds to the maximum center-peak intensity.

Figure 7 shows the superresolution effect of the proposed method and the phase-shifting method ($b=0$). It is easy to see that when the half-width ratio equals 0.744, the proposed method and the phase-shifting method have the

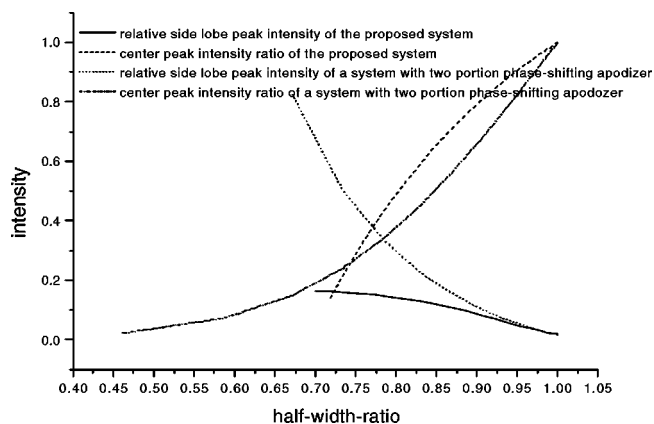


Fig. 7 Center-peak intensity ratio and first sidelobe intensity versus half-width ratio of the proposed method and the phase-shifting method.

same center-peak intensity of 0.257, but the sidelobe of the phase-shifting method is too high. When the half-width ratio is larger than 0.744, the proposed method has a higher center-peak intensity and a lower sidelobe than the phase-shifting method. When the half-width ratio is smaller than 0.744, the proposed method has a lower center-peak intensity. Does that mean that the phase-shifting method has some advantage over the proposed method?

The answer is no. Because the sidelobe intensity of the phase-shifting method is very high, we tried to optimize the apodizer by adjusting the inner radius b and outer radius a , but when the first sidelobe was lowered, the second sidelobe would increase. In Fig. 7, for a half-width ratio of 0.7177, the proposed method has a center-peak intensity of 0.1363 and a relative sidelobe intensity of 0.162, and the phase-shifting method has a center-peak intensity of 0.2157 and a relative sidelobe intensity of 0.5760. When the relative sidelobe intensity is reduced to 0.1700, the second-sidelobe intensity is 0.4700, the center-peak intensity is 0.1296, and the half-width ratio is 0.7373. Now we can see that the superresolution effects of the proposed method are still superior to those of the optimized phase-shifting apodizer. The proposed method has a superresolution limit of half-width ratio=0.700

Figure 8 shows the profiles of the superresolution effects of an optical system with an optimized three-part phase-shifting apodizer and one with the proposed apodizer. The three-part apodizer is optimized for data storage. We assume that the acceptable minimum value of the center-peak intensity ratio is 0.3, and the acceptable maximum relative sidelobe intensity is 0.2. The dashed curve corresponds to a system with a phase-shifting apodizer, and the solid curve corresponds to the system with the proposed apodizer. With a center-peak intensity ratio of 0.303, the phase-shifting system has a half-width ratio of 0.795 and a relative sidelobe intensity of 19.7%, while the one with the proposed apodizer has a center-peak intensity of 0.323, a half-width ratio of 0.758, and a relative sidelobe intensity of 15.5%. The sidelobe of the curve created with three-part phase-shifting method might be brought down by increasing the inner radius b , but the half-width ratio would then be larger. An increase in the number of parts would decrease

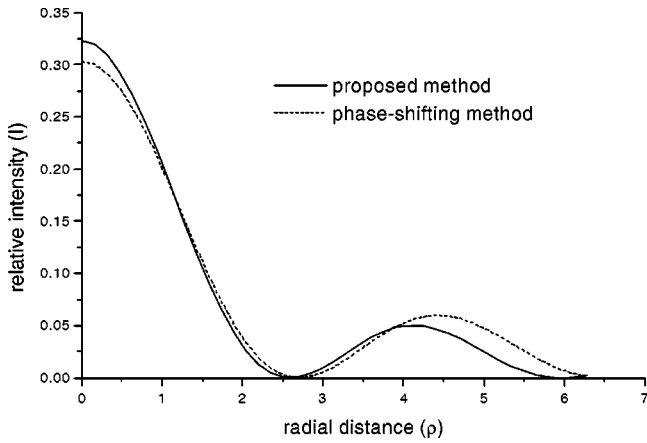


Fig. 8 Comparison of the performance of the new apodizer with that of the optimized three-part phase-shifting apodizer. The dashed curve corresponds to a system with phase-shifting apodizer, and the solid curve corresponds to the system with the proposed apodizer.

the half-width ratio, but the center peak intensity would then decrease rapidly.

5 Conclusion

In summary, we have proposed a new way to gain super-resolution by modifying the spatial frequency of the inner part of the beam. Simulation results have shown that it has better performance than the phase-shifting method and the center-obstruction method. (Actually, any increase in the statistical spatial frequency will result in the improvement of resolution; this will be shown in a future publication.) Although it is possible to design diffractive elements that accomplish the conversion to an annular beam, that method should be used with care, because the efficiency cannot be 100% and there is always a phase associated with the annular beam even if one of the diffractive elements corrects for it in the near field.

6 Appendix

The power series for the Bessel function is

$$\begin{aligned}
 J_1(z) &= \frac{z}{2} \sum_{n=0}^{\infty} \frac{(-1)^n (z/2)^{2n}}{n!(n+1)!} \\
 &= 2.0 \frac{z}{4} - 4 \left(\frac{z}{4}\right)^3 + 2.7 \left(\frac{z}{4}\right)^5 - 0.89 \left(\frac{z}{4}\right)^7 + 0.18 \left(\frac{z}{4}\right)^9 \\
 &\quad - \dots
 \end{aligned} \tag{a}$$

Acknowledgments

The authors would like to thank Professor Wendong Xu and Xiaoqiang Deng for helpful discussions. The Chinese Academy of Sciences Project No. KJ951-B1-702-03, "High Density Optical Data Storage," supports this work.

References

1. I. J. Cox and C. J. R. Sheppard, *J. Opt. Soc. Am. A* **3**(8), 1152 (1986).
2. T. R. M. Sales and G. M. Morris, *Opt. Lett.* **22**(9), 582 (1997).
3. T. R. M. Sales and G. M. Morris, *J. Opt. Soc. Am. A* **14**(7), 1637 (1997).
4. H. Ando, *Jpn. J. Appl. Phys.* **31**, 557 (1992).
5. I. J. Cox and C. J. R. Sheppard, *J. Opt. Soc. Am.* **72**(9), 1287 (1982).
6. A. J. den Dekker and A. van den Bos, *J. Opt. Soc. Am. A* **14**(3), 547 (1997).
7. C. W. McCutchen, *J. Opt. Soc. Am.* **57**(10), 1190 (1967).
8. W. Lokosz, *J. Opt. Soc. Am.* **54**, 1463 (1966).
9. G. Jin, "Beam Shaping," (in Chinese), in *Binary Optics*, p. 233, National Defense and Industrial Press (1998).
10. M. T. Eismann, A. M. Tai, and J. N. Cederquist, *Appl. Opt.* **28**(13), 2641 (1989).
11. S. Sinzinger, K. H. Brenner, J. Moisel, T. Spick, and M. Testorf, *Appl. Opt.* **34**(29), 6626 (1995).
12. W. T. Welford, *J. Opt. Soc. Am.* **50**(8), 749 (1960).



Haifeng Wang received his BS degree in physics in 1995 and then his MS in optics from Soochow University. He is now a doctoral student in the Shanghai Institute of Optics and Fine Mechanics, Chinese Academy of Sciences. He has published about 10 papers. His research interests include phase-shifting techniques, optical data storage, optical information processing, optical superresolution techniques, interferometry, biomedical imaging, and spectroscopy.

Fuxi Gan: Biography not available.